Modulation of receptor cycling by neuron-enriched endosomal protein of 21 kD

Pascal Steiner,[1,2] J.-C. Floyd Sarria,[1,2] Liliane Glauser,[1,2] Sarah Magnin,[1,2] Stefan Catsicas,[1] and Harald Hirling[1,2]

[1]Faculté des Sciences de la Vie, Ecole Polytechnique Fédérale de Lausanne, 1015 Lausanne, Switzerland
[2]Institut de Biologie Cellulaire et de Morphologie, 1005 Lausanne, Switzerland

Although correct cycling of neuronal membrane proteins is essential for neurite outgrowth and synaptic plasticity, neuron-specific proteins of the implicated endosomes have not been characterized. Here we show that a previously cloned, developmentally regulated, neuronal protein of unknown function binds to syntaxin 13. We propose to name this protein neuron-enriched endosomal protein of 21 kD (NEEP21), because it is colocalized with transferrin receptors, internalized transferrin (Tf), and Rab4. In PC12 cells, NEEP21 overexpression accelerates Tf internalization and recycling, whereas its down-regulation strongly delays Tf recycling. In primary neurons, NEEP21 is localized to the somatodendritic compartment, and, upon N-methyl-D-aspartate (NMDA) stimulation, the alpha-amino-3-hydroxy-5-methyl-4-isoxazolepropionate receptor subunit GluR2 is internalized into NEEP21-positive endosomes. NEEP21 down-regulation retards recycling of GluR1 to the cell surface after NMDA stimulation of hippocampal neurons. In summary, NEEP21 is a neuronal protein that is localized to the early endosomal pathway and is necessary for correct receptor recycling in neurons.

Introduction

Endosomes are key sorting organelles in eukaryotic cells. Because they receive endocytosed lipids and proteins from the plasma membrane they are directly involved in its remodeling. Endocytic vesicles fuse with early endosomes (EEs)*. There, molecules are directed either to late endosomes for degradation, or are recycled back to the plasma membrane via a direct route or indirectly through tubular vesicular recycling endosomes (REs) (Gruenberg and Maxfield, 1995). Although the precise steps involved are still elusive, members of the Rab family of small GTPases can demarcate subdomains of the engaged endosomes, as they are implicated in specific endosomal trafficking steps (Gorvel et al., 1991; van der Sluijs et al., 1992; Ullrich et al., 1996; Trischler et al., 1999; Sonnichsen et al., 2000).

Internalization and insertion of membrane proteins in a temporally and spatially ordered manner is extremely important during neuronal differentiation and in adult neurons. Endosomal organelles have been identified in growth cones of developing neurons (Dailey and Bridgman, 1993; Diefenbach et al., 1999). The role of endosomal protein recycling for signal transduction during development has been shown in a number of cases, including the cell adhesion molecule L1 (Kamiguchi and Lemmon, 2000) and the high-affinity nerve growth factor receptor TrkA (Grimes et al., 1996). Likewise, γ-aminobutyric acid receptors (Wan et al., 1997) are recruited from internal compartments during insulin stimulation in adult neurons. In addition, recent studies indicate a rapid alpha-amino-3-hydroxy-5-methyl-4-isoxazolepropionate (AMPA) receptor cycling through endosomes during synaptic transmission and plasticity (Carroll et al., 1999; Beatti et al., 2000; Ehlers, 2000; Lin et al., 2000), and a switch between different AMPA receptor subunits during synaptogenesis (Pickard et al., 2000; Zhu et al., 2000).

Endosomal trafficking implies docking and fusion of transport vesicles. This depends on SNARE (Rothman, 1994). Syntaxin 13 is a SNARE localized to REs (Prekeris et al., 1998; Tang et al., 1998; Hirling et al., 2000). Antibody blocking of syntaxin 13 in permeabilized cells inhibited transferrin (Tf) release, suggesting that it acts on a recycling compartment (Prekeris et al., 1998). Such antibodies also inhibited in vitro EE fusion, and syntaxin 13 forms a

complex with the Rab5 effector proteins EEA1 and Rabaptin-5 (McBride et al., 1999). We have previously identified syntaxin 13 from early postnatal brain as a copurifying band on an anti–SNAP-25 immunocolumn. We have also shown that syntaxin 13 is strongly expressed in developing brain and enhances neurite outgrowth in PC12 cells (Hirling et al., 2000), suggesting an important role of the endocytic pathway during neuronal development.

Despite the morphological characterization of endosomes in neurons and their importance in receptor cycling, little is known about specific neuronal proteins involved in this process. The strong expression of syntaxin 13 during development and its outgrowth-enhancing effect prompted us to search for syntaxin 13–binding proteins from developing brain. Here we describe that neuron-enriched endosomal protein of 21 kD (NEEP21) is in a complex with syntaxin 13. NEEP21 has previously been cloned as a neuron-enriched, developmentally regulated membrane protein called 1A75 (Sutcliffe et al., 1983) or p21 (Saberan-Djoneidi et al., 1998) whose function has been unknown. We now show that it localizes to Rab4-positive endosomes in the somatodendritic neuronal compartment. Its overexpression accelerates, whereas down-regulation strongly delays Tf and L1 recycling. Finally, we also show that upon N-methyl-D-aspartate (NMDA) stimulation of hippocampal neurons, AMPA receptors are internalized into NEEP21-positive compartments, and that recycling of AMPA receptors is delayed by NEEP21 down-regulation.

Results

NEEP21 forms a complex with syntaxin 13

To investigate endocytic mechanisms during neuronal differentiation, we immunopurified syntaxin 13–binding proteins specifically enriched in developing brain. Membrane extracts from postnatal day (P)3 or adult rat brain were sequentially passed over a nonspecific IgG column and a specific anti–syntaxin 13 column. Several nonspecific proteins, including tubulin, appeared in the elutions (Fig. 1 A). In agreement with our previous finding (Hirling et al., 2000), we detected syntaxin 13 at 38 kD with a lower intensity from adult than from postnatal brain (Fig. 1 A; unpublished data). From P3 extract we identified a specific band at 21 kD (arrowheads). Microsequencing identified two peptides, with the major one being SVSPWMSV. Database searches revealed that it is contained in the brain-specific rat clone 1A75 (Sutcliffe et al., 1983), and in a recently cloned mouse full-length 1A75/p21 (Saberan-Djoneidi et al., 1998). With the exception of a low expression in testis, 1A75/p21 mRNA is neuron specific and developmentally regulated (Sutcliffe et al., 1983; Saberan-Djoneidi et al., 1998), but the function of this protein remains unknown. We have cloned, by PCR, a cDNA coding for the 185 amino acids (aa) of full-length 1A75 from mouse total brain cDNA. Based on the results of the present study, we propose the name NEEP21. We raised a polyclonal antibody against a peptide spanning aa 7–23. It recognized a single band at 21 kD (Fig. 1 B, lanes b and c) which is not present using either preimmune serum (lane a), or purified antibody preblocked with peptide (lane d).

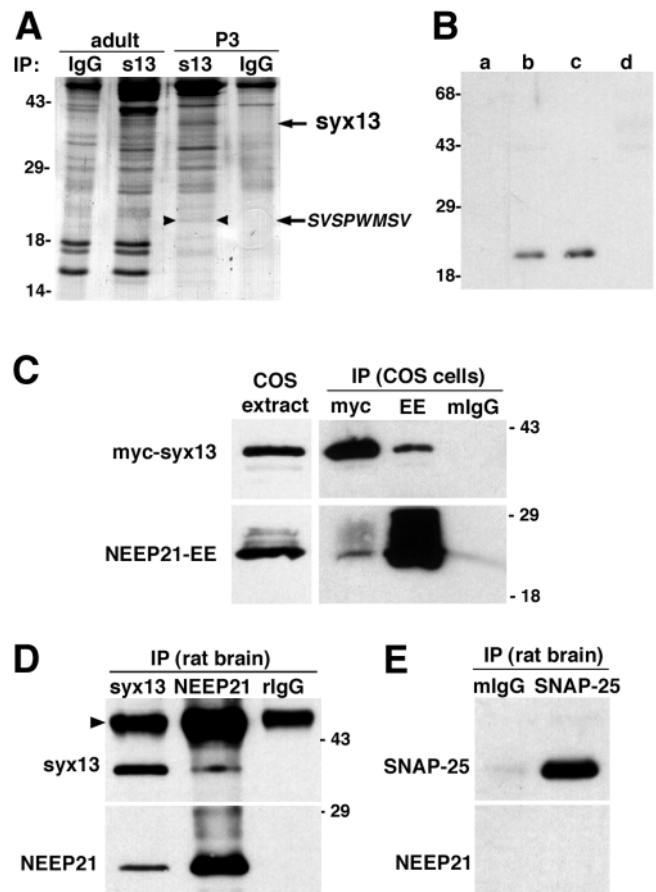To verify that syntaxin 13 and NEEP21 can form a complex, we cotransfected myc-tagged syntaxin 13 and EE-

Figure 1. **NEEP21 forms a complex with syntaxin 13.** (A) Membrane extracts from P3 or adult rat brain were sequentially passed over rabbit IgG- and anti–syntaxin 13 (s13) columns. Eluted proteins were separated on SDS-PAGE stained with Coomassie blue. The 21-kD band (arrowheads) contained the indicated peptide sequence. (B) Immunoblot of P3 rat brain extract (30 μg) using a polyclonal anti-NEEP21 antibody. Lane a, preimmune serum; lane b, crude immune serum; lane c, affinity-purified antibody; lane d, purified antibody blocked by antigenic peptide. (C) COS-7 cells cotransfected with myc-tagged syntaxin 13 and EE-tagged NEEP21. Shown is the COS extract and IP with monoclonal anti-myc, anti-EE, or mouse IgG. Detection on blots used anti–syntaxin 13 or -NEEP21 antibodies. (D) Membrane extracts from P3 rat brain were subjected to IP using polyclonal anti-syntaxin 13, anti-NEEP21, or rabbit IgG. There are crossreacting antibody heavy chains (arrowhead) as the same antibodies were used for immunoblots. (E) As in D, but using mouse IgG or monoclonal anti-SNAP-25 antibodies for IP, and polyclonal anti-SNAP-25 and anti-NEEP21 antibodies for blot. Molecular weights are indicated in kD.

tagged NEEP21 into COS-7 cells. NEEP21-EE appeared in the extract as a major band at its corresponding size with a few slightly higher migrating minor bands (Fig. 1 C). Both anti-myc and -EE antibodies, but not IgG, coprecipitated myc-syntaxin 13 and NEEP21-EE (Fig. 1 C). Next, we immunoprecipitated endogenous syntaxin 13 and NEEP21 from P3 rat brain membrane extracts (Fig. 1 D). Anti–syntaxin 13 beads precipitated syntaxin 13 and coprecipitated NEEP21. Vice versa, anti-NEEP21 beads precipitated NEEP21 and coprecipitated syntaxin 13. Control IgG beads did not precipitate either protein. The substoichiometric bands after precipitation suggest that only subpopulations of both proteins are in a complex at steady state. Because we
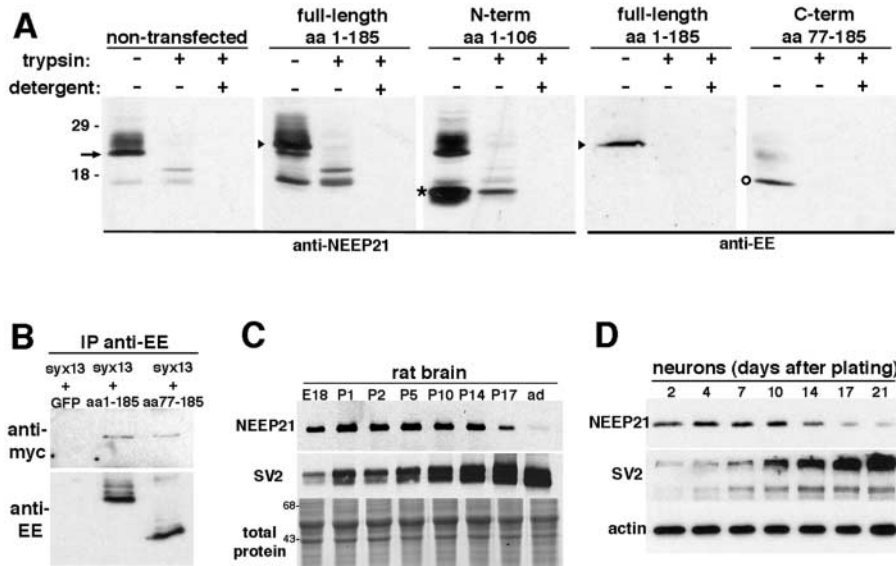
Figure 2. **Membrane topology of NEEP21.** (A) Membrane fragments (40 μg) of nontransfected PC12 cells, or cells transfected with full-length NEEP21 (1–185; arrowhead), its NH$_2$ terminus (aa 1–106; asterisk), or its COOH terminus (aa 77–185; ○) were incubated without or with 4 μg trypsin and 0.5% Triton X-100. Western blots probed with anti-NEEP21 (NH$_2$-terminal epitope) or anti-EE (COOH-terminal epitope) are shown. (B) Immune pellets after IPs from COS-7 cells transfected with myc–syntaxin 13 and either GFP, full-length NEEP21-EE, or NEEP21-aa77–185-EE (missing NH$_2$ terminus). Anti-EE and anti-myc were used on blot. (C) Immunoblot of rat brain extracts (30 μg) at different developmental stages (E, embryonic day; ad, adult) probed using anti-SV2 and -NEEP21 antibodies. A parallel Coomassie blue–stained gel (total protein) indicates equal loading. (D) Immunoblot of extracts from rat cortical neuron cultures (30 μg) at the indicated ages, probed with anti-SV2, -actin and -NEEP21 antibodies.

originally identified syntaxin 13 on an anti–SNAP-25 column (Hirling et al., 2000), we also precipitated with anti–SNAP-25 antibodies (Fig. 1 E). No NEEP21 was detected, suggesting that syntaxin 13 forms separate complexes with SNAP-25 and NEEP21.

Analysis of the NEEP21 primary sequence suggested a hydrophilic NH$_2$-terminal domain (aa 1–84), one transmembrane region (aa 85–103), and a hydrophilic COOH-terminal domain (aa 106–185) (Saberan-Djoneidi et al., 1998). To analyze its membrane orientation, membrane fractions of nontransfected PC12 cells, or cells transfected with either full-length NEEP21-EE (aa 1–185), its NH$_2$ terminus (aa 1–106), or its COOH terminus (aa 77–185), were analyzed using antibodies recognizing the NH$_2$ (anti-NEEP21) or COOH terminus (anti-EE) (Fig. 2 A). Without trypsin digestion, anti-NEEP21 recognized endogenous NEEP21 (arrow) as well as transfected full-length protein (arrowhead) and the NH$_2$ terminus (asterisk). In addition, a potential degradation product at ∼17 kD was detected. Upon trypsin digestion, endogenous and transfected full-length proteins were not detectable, whereas the 17-kD band and an additional degradation band appeared. In contrast, the transfected NH$_2$ terminus was detectable at the same size before or after digestion (asterisk). The weaker bands after digestion can be explained by organelles that did not stay sealed upon cell breakage. Trypsin incubation in the presence of detergent, which lyses organelle membranes, erased all bands (Fig. 2 A). These data indicated that the NH$_2$-terminal domain is protected by membranes. In cells transfected with full-length NEEP21-EE (arrowhead) or its COOH terminus (○), anti-EE recognized both proteins, but no protected fragments remained after digestion with or without detergent (Fig. 2 A). Taken together, these results suggested that the COOH terminus is oriented toward the cytosol, whereas the NH$_2$ terminus is on the lumenal side of organelle membranes. Because no labeling was observed in anti-NEEP21 immunostainings in the absence of detergent (unpublished data), it is unlikely that a significant fraction is localized to the plasma membrane. To analyze whether a NEEP21 mutant lacking the NH$_2$-terminal lumenal tail is able to form a complex with syntaxin 13, COS-7 cells were cotransfected with myc–syntaxin 13 and either full-length NEEP21-EE or aa 77–185-EE. Indeed, anti-EE coprecipitated in both cases syntaxin 13 (Fig. 2 B).

Because we detected NEEP21 only from postnatal brain, we investigated NEEP21 levels during brain development. In agreement with our affinity purification and previous Northern blot analysis (Saberan-Djoneidi et al., 1998), NEEP21 was strongly detected around birth, and then decreased at ∼P14 (Fig. 2 C). This pattern is also similar to the one of syntaxin 13 (Hirling et al., 2000). In contrast, synaptic vesicle protein (SV)2 increased during the first two postnatal weeks. To correlate this developmental profile with differentiation in dissociated neurons, we investigated NEEP21 levels in cortical neuronal cultures at different stages (Fig. 2 D). SV2 increased during the investigated 3 wk, whereas NEEP21 was already strongly detected on day 2, and started to decline at around day 14. We also confirmed the reported neuronal expression of NEEP21 mRNA (Sutcliffe et al., 1983; Saberan-Djoneidi et al., 1998) at the protein level using extracts of mouse cortical neuron and astrocyte cultures (unpublished data). Together, these data indicate that NEEP21 is strongly expressed in neurons during maturation and synapse formation.

NEEP21 is detected in Tf- and Rab4-positive, wortmannin-sensitive endosomes

Next, we analyzed the localization of NEEP21 by immunofluorescence. In differentiated PC12 cells, endogenous (Fig. 3 A) as well as transfected EE-tagged (Fig. 3 D) NEEP21 local-

Figure 3. **NEEP21 localizes to EEs in PC12 cells.** (A–F) PC12 cells were transfected with myc–syntaxin 13 (A–C) or NEEP21-EE (D–F) followed by NGF differentiation for 2 d and immunolabeling using antibodies against NEEP21 (A), myc (B), EE (D), or TGN38 (E). Note partial colocalization of NEEP21 with syntaxin 13 in inserts of A–C. (G–L) PC12 cells transfected with human TfR were incubated on ice with human FITC-Tf, and subsequently at 37°C without Tf for 3 (H) or 15 min (K), and immunostaining for NEEP21 (G and J). (M–O) PC12 cells were immunolabeled for NEEP21 (M) and the late endosome-enriched phospholipid LBPA (N). Bars, 20 μm. Single confocal sections are presented. Overlays are on the right panel.
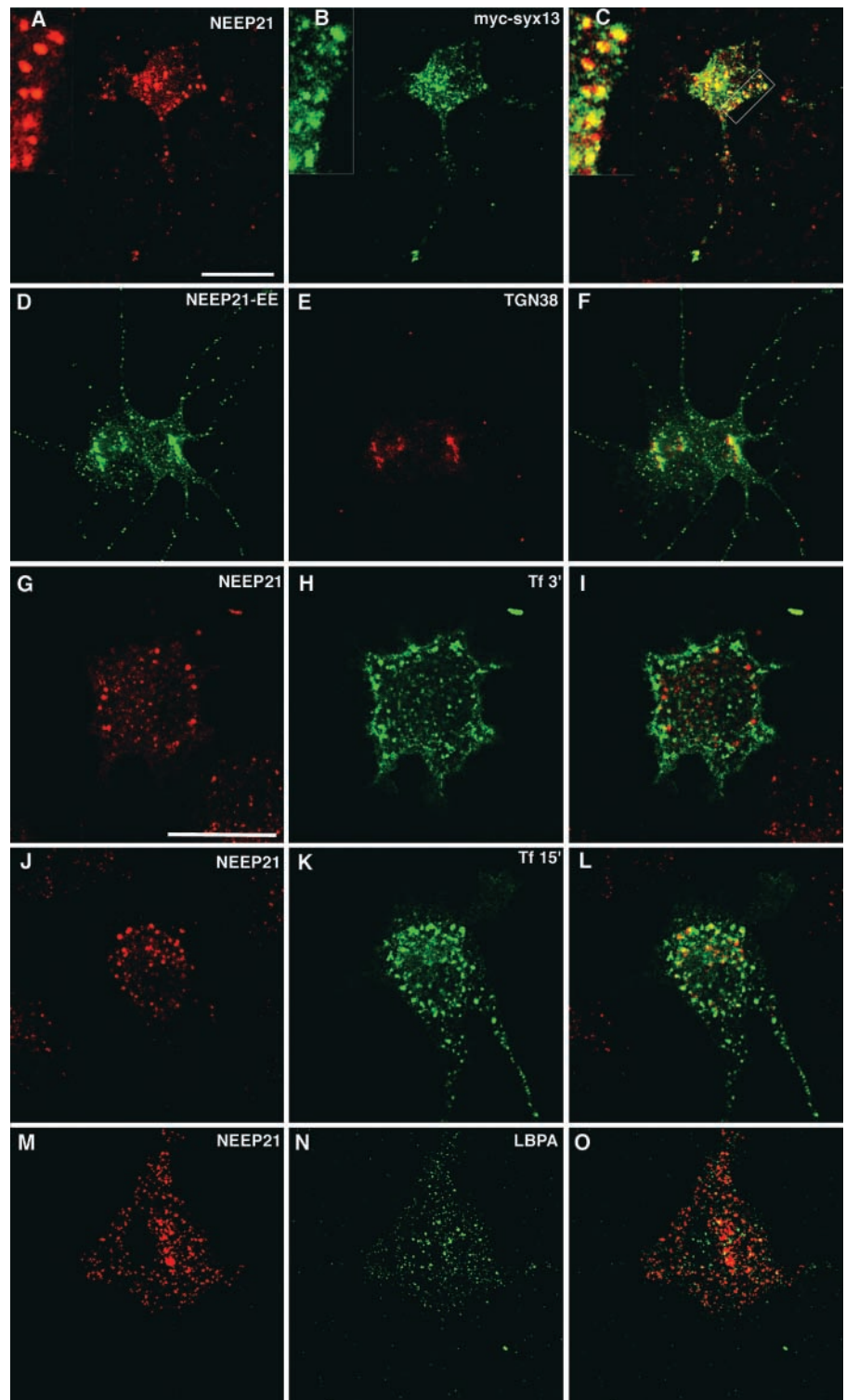
ized to puncta in the cell body and along neurites. There is a significant colocalization with the less regularly shaped myc–syntaxin 13-labeled organelles (Fig. 3, B, overlay in C, and compare inserts in A–C). Overlap between transfected NEEP21-EE (Fig. 3 D) and trans-Golgi network (TGN)38 (Fig. 3 E) is limited to the perinuclear region. Due to the coprecipitation with syntaxin 13, we tested for an endosomal localization of NEEP21. We internalized Tf as a marker of the endosomal recycling pathway. PC12 cells with prebound surface FITC-labeled Tf were incubated for 3 or 15 min to

allow Tf endocytosis (Fig. 3, H and K). At 3 min, labeled peripheral endosomes colocalized rarely with NEEP21 puncta (Fig. 3, G and overlay in I), whereas at 15 min, the majority of signals indicated colocalization (Fig. 3, J, K, and overlay in L). Because at 3 min Tf should localize to endocytic vesicles transported to or fusing with EEs, NEEP21 is primarily associated with Tf-positive compartments beyond the transport to EEs. To analyze whether NEEP21 also localizes to late endosomes, we costained PC12 cells for NEEP21 (Fig. 3 M) and lysobisphosphatidic acid (LBPA) (Fig. 3, N and overlay
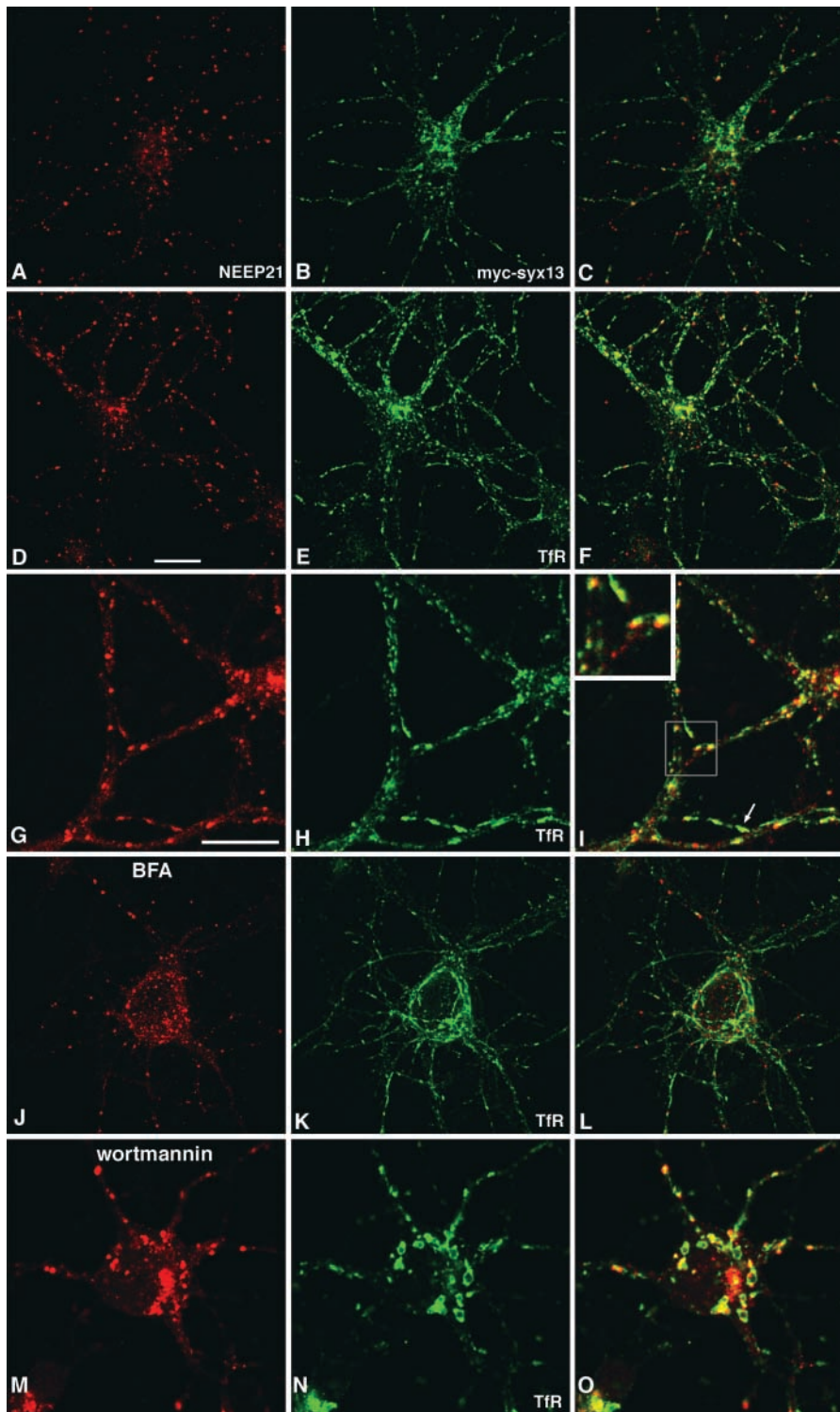
Figure 4. **Localization of NEEP21 in neurons and redistribution by BFA and wortmannin.** (A–C) Cortical neurons transfected with myc–syntaxin 13 were immunostained at DIV10 using anti-NEEP21 (A) and anti-myc (B and overlay in C). (D–O) Untreated cortical neurons at DIV3 (D–I), or treated for 60 min with 5 μg/ml BFA (J–L), or with 100 nM wortmannin (M–O) were immunostained for NEEP21 (D, G, J, and M) and TfR (E, H, K, and N). Overlays in F, I, L, O. Bars 20 μm.

in O), a phospholipid enriched in late endosomes (Kobayashi et al., 1998). No colocalization was observed, ruling out a late endosomal localization of NEEP21. These results indicate that NEEP21 localizes to EEs or REs.

Similar to the pattern in PC12 cells, NEEP21 localized in cortical neurons to distinct puncta (Fig. 4, A, D, and G), which colocalized partially with transfected myc–syntaxin 13 (Fig. 4, B and overlap in C). We verified by costaining for the transferrin receptor (TfR) (Fig. 4, E and H), that NEEP21 also localizes in primary neurons to TfR/Tf-positive endosomes. We

found most NEEP21 puncta overlapping with (Fig. 4 I, arrow) or in close apposition to (Fig. 4 I, enlarged area) TfR-positive endosomes. TfR-positive organelles can correspond to EEs and REs. To distinguish which are positive for NEEP21, we applied the drugs brefeldin A (BFA) and wortmannin. BFA causes tubulation of Tf-positive compartments (Lippincott-Schwartz et al., 1991; Tooze and Hollinshead, 1992), which are mainly Rab4/Rab11-positive, suggesting that BFA acts on a late step of recycling (Sonnichsen et al., 2000). When we treated neurons with BFA, TfR was observed in a tubule-like staining (Fig. 4 K)

Figure 5.   **NEEP21 colocalizes with Rab4 and Rab5Q79L, but rarely with wild-type Rab5, Rab11, and EEA1.** PC12 cells, transfected with myc-tagged wild-type Rab5 (A–C), Rab5-Q79L (J–L), or nontransfected cells (D–I and M–O) were labeled with anti-NEEP21 (left) and either anti-myc (B and K), -Rab4 (E), -Rab11 (H), or -EEA1 (N) antibodies. Overlays on the right panel. Bar, 10 μm. Single confocal sections are shown.
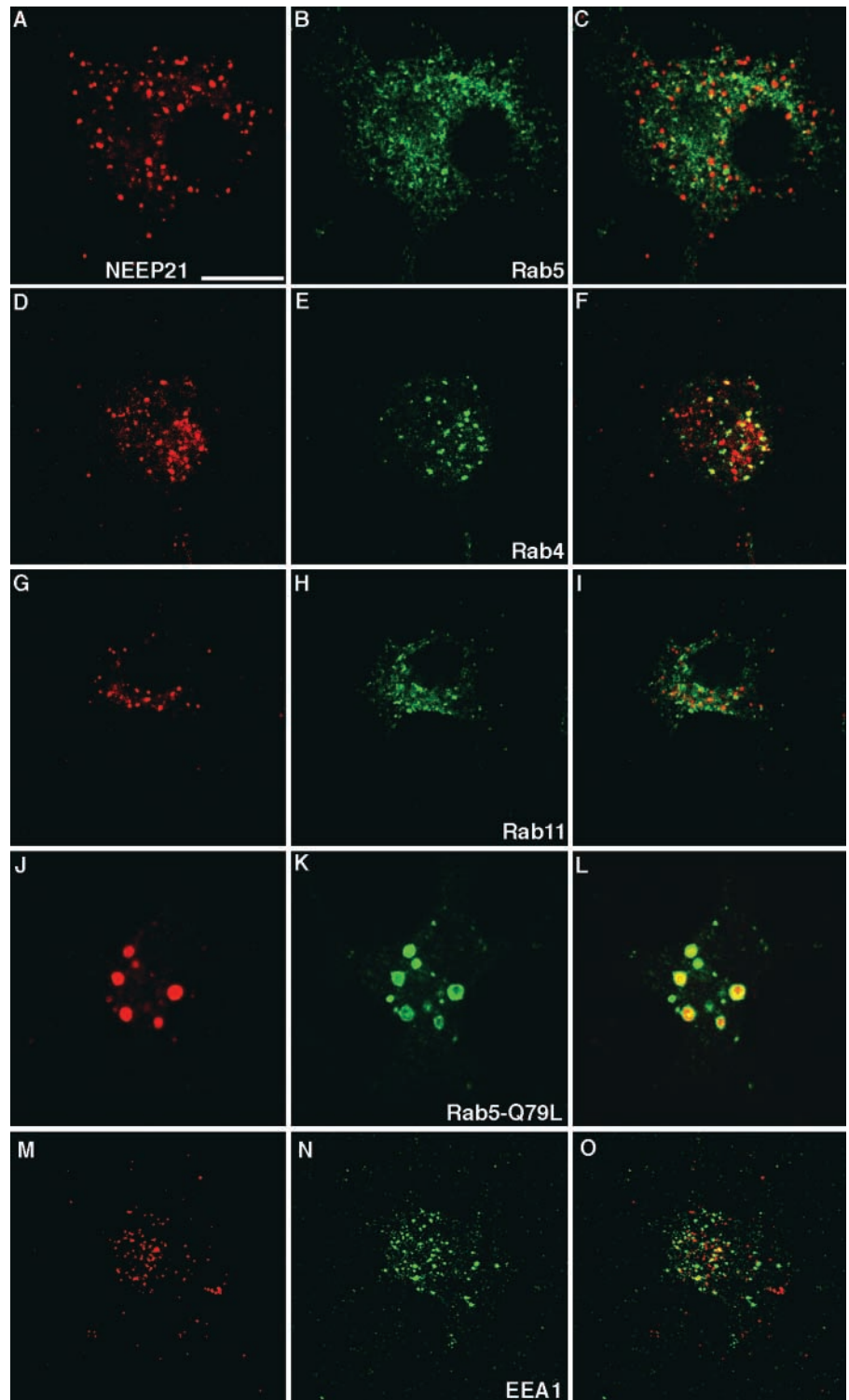
compared with control cells (Fig. 4, E and H). The NEEP21-positive puncta (Fig. 4 J) appeared slightly more diffuse than in controls, and rarely colocalized with TfR (Fig. 4, compare L and F), suggesting that NEEP21 is mainly on BFA-insensitive endosomes. Wortmannin causes enlarged Tf-positive structures (Spiro et al., 1996; Malide and Cushman, 1997) that colocalize mainly with Rab5/Rab4 corresponding to an early or intermediate recycling step (Sonnichsen et al., 2000). In neurons treated with wortmannin, TfR was detected in patchy disk-like structures (Fig. 4 N). NEEP21 localized to enlarged irregular puncta (Fig. 4 M) that overlapped strongly with the TfR-positive patches (Fig. 4 O). This shows that NEEP21 localizes to a wortmannin-sensitive endosomal compartment.

To localize NEEP21 more precisely along the early endosomal pathway, we immunolabeled PC12 cells for Rab4, Rab5, Rab11, and EEA1. The discrete NEEP21 puncta (Fig. 5, left) rarely colocalized with compartments positive for myc-Rab5 (Fig. 5, B and overlay in C). In contrast, there was a significant colocalization between NEEP21 and Rab4 (Fig. 5, D–F). In immunostainings for NEEP21 and Rab11,
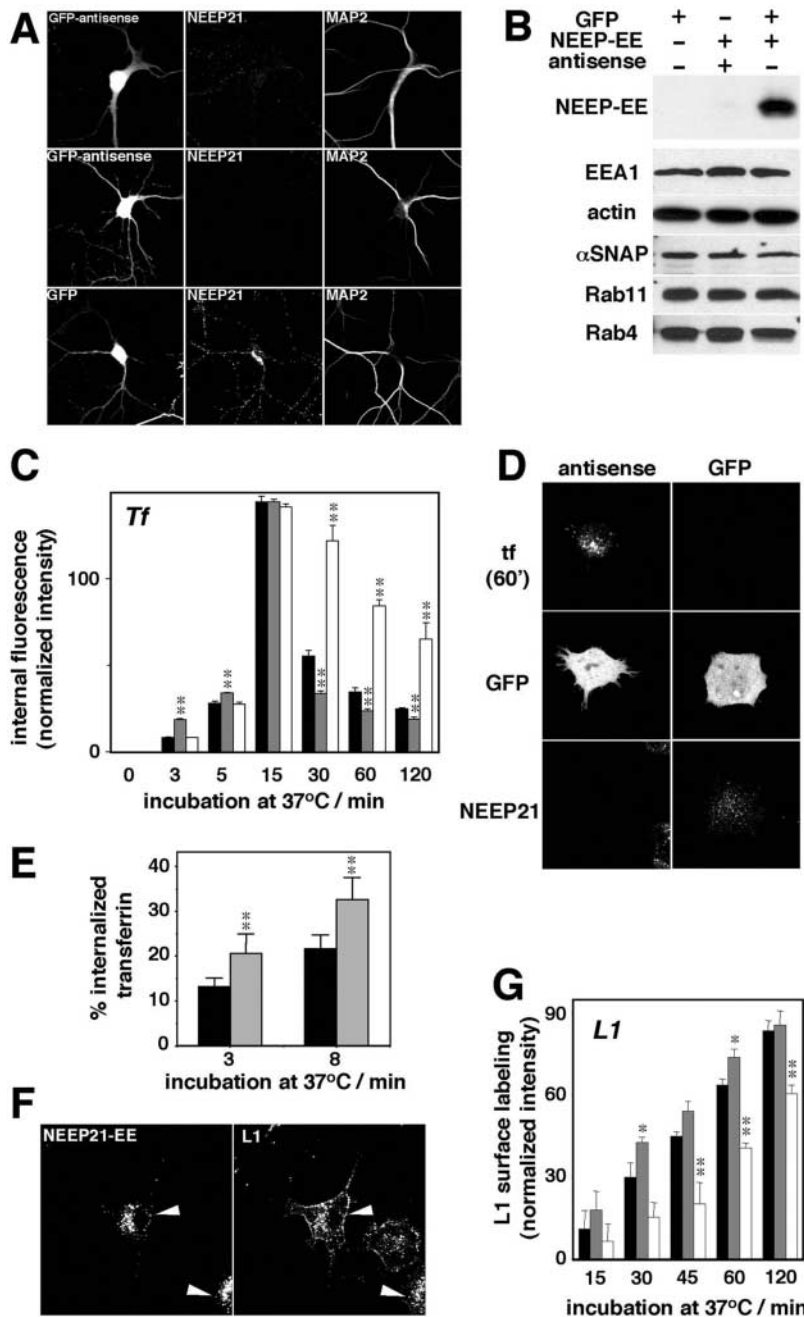
Figure 6.   **NEEP21 modulates Tf and L1 cycling.** (A) NEEP21 reverse cDNA downstream of the GFP open-reading frame (top and middle rows), or GFP alone (bottom row) were transfected into hippocampal neurons. NEEP21 staining (middle) is strongly reduced in GFP-antisense–transfected cells compared with the GFP-transfected cell; MAP2 staining on the right panel. (B) Western blot from COS-7 cells cotransfected with the indicated cDNAs. Antisense abolishes NEEP21 expression, while endogenous proteins are not affected. (C) PC12 cells, cotransfected with human TfR and either GFP (black bars), NEEP21-EE (gray bars), or antisense (white bars), were incubated on ice with rhodamin-Tf, and subsequently at 37°C without Tf for the indicated times. Acid-washed cells were immunolabeled for NEEP21. Tf fluorescence on confocal images was quantified. Significant differences by NEEP21 overexpression or suppression compared with GFP are indicated by double asterisks ($P < 0.01$). Error bars indicate SEM. (D) Typical cells transfected with GFP-antisense (left) or GFP (right) as in C at 60 min (E) HIT-T15 cells, cotransfected with TfR and either vector (black bars) or NEEP21-EE (gray bars), were incubated with HRP-Tf on ice, and then without HRP-Tf at 37°C for 3 or 8 min. Peroxidase activity in extracts of acid-washed cells revealed significant increases of Tf endocytosis by NEEP21-EE at 3 and at 8 min compared with control cells ($P < 0.001$). Error bars indicate SD. (F) Colocalization of NEEP21 with L1; see structures indicated by arrowheads. (G) PC12 cells, transfected as in C (without TfR), were surface labeled at 0 min using an anti-L1 antibody against an extracellular epitope and Cy5 secondary IgG, and then incubated for the indicated times. Cells were fixed and again surface labeled for L1 and Cy3 secondary IgG to label newly inserted L1. Significant effects compared with controls are indicated with single ($P < 0.02$) or double ($P < 0.01$) asterisks. Error bars indicate SEM.

a few colocalizing signals were observed (Fig. 5, G–I). The GTPase-deficient mutant Rab5-Q79L causes enlargement of EEs due to increased fusion of endocytic vesicles (Stenmark et al., 1994). We found a complete overlap between endogenous NEEP21 (Fig. 5 J) and transfected Rab5Q79L (Fig. 5, K and overlay in L) in these enlarged organelles. Little colocalizing signals were observed between NEEP21 (Fig. 5 M) and EEA1 (Fig. 5 N). Taken together, these data indicate that NEEP21 localizes mainly to Rab4-positive, Rab5/EEA1-negative, wortmannin-sensitive endosomes.

Overexpression or suppression of NEEP21 modulates Tf cycling

We next tested whether changing NEEP21 expression affects receptor cycling. For its suppression, we constructed a plasmid carrying the NEEP21 cDNA in reverse direction, downstream of the green fluorescent protein (GFP) open-reading frame. This yields an RNA for translation of GFP and hybridization to endogenous NEEP21-coding RNA. When transfected into cortical neurons, NEEP21 staining (Fig. 6 A, middle) is clearly decreased in GFP-antisense–positive cells (top and middle rows) compared with the GFP-transfected cell (bottom row). Staining for MAP2 was indistinguishable (right). Because immunoblots of endogenous NEEP21 in such neurons or PC12 cells were not possible because of low transfection efficiency, we used transfected COS-7 cells. Cotransfection of NEEP21-EE and GFP yielded a strong NEEP21-EE expression (Fig. 6 B, right lane). In contrast, upon cotransfection of NEEP21-EE and antisense, NEEP21 expression was specifically inhibited (Fig. 6 B, middle lane),

Figure 7. **NEEP21 localizes to the somatodendritic compartment.** Hippocampal neurons at DIV10 were double labeled using antibodies against NEEP21 (A, D, G, J, and M), MAP2 (B), Tau (E), SNAP25 (H), SV2 (K), or synaptophysin (N). Overlays on the right panel. Marked areas in J, K and M, and N are enlarged in L and O, respectively. Bars, 20 μm.
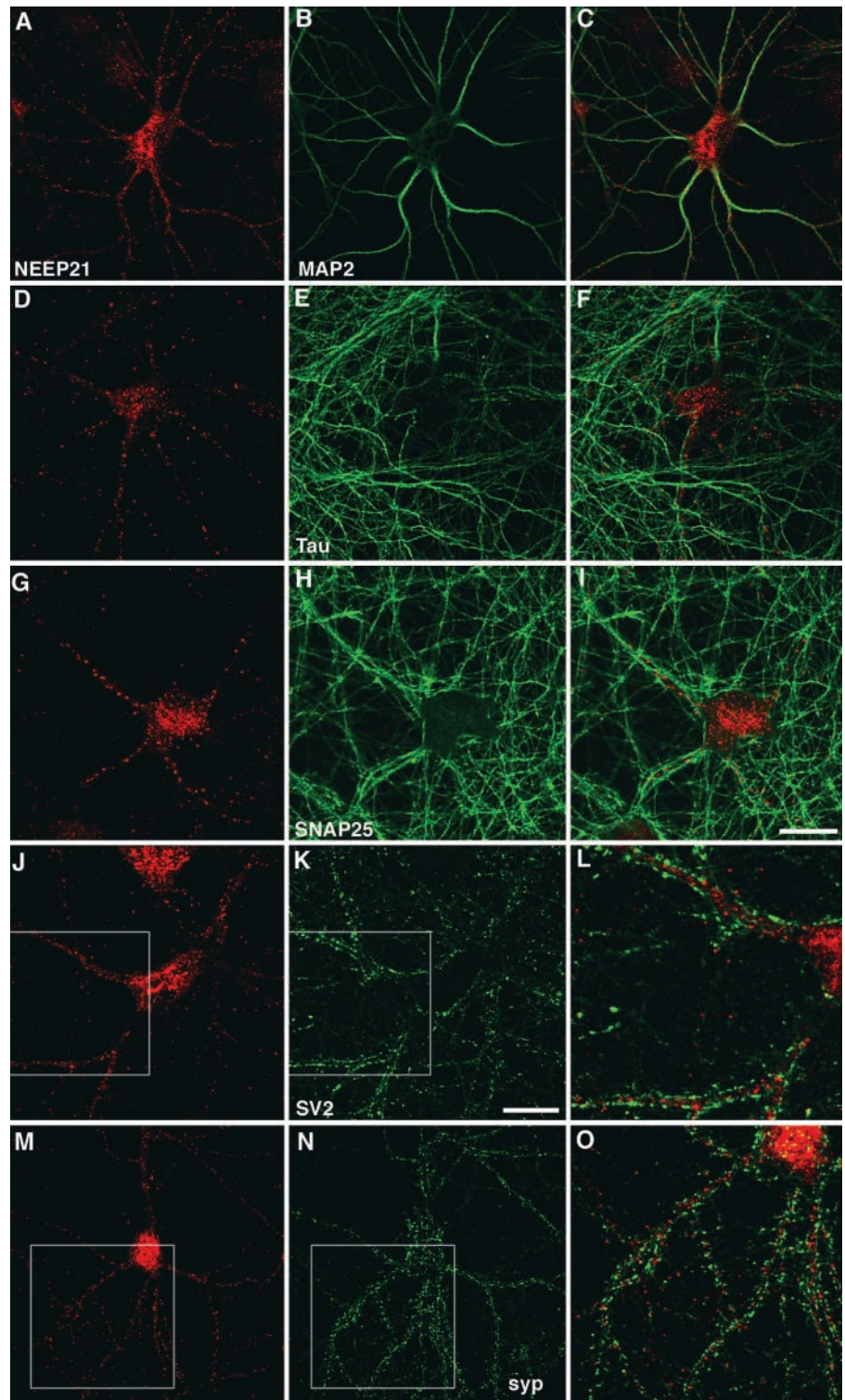
whereas nonrelated EEA1, actin, αSNAP, Rab11, and Rab4 were not affected. Therefore, we used the antisense plasmid to analyze the effect of NEEP21 suppression on receptor cycling.

Transfected PC12 cells expressing human TfR and either GFP (control), antisense (suppression), or NEEP21-EE (overexpression) were preincubated on ice with rhodamin-conjugated human Tf, followed by incubation at 37°C without Tf. External Tf was removed by acid stripping, and suppression of NEEP21 verified by immunocytochemistry.

Fluorescence of internalized Tf was quantified on confocal sections. Tf labeling of GFP-transfected cells corresponded to a typical time course of Tf internalization/recycling with a maximal internal accumulation at 15 min (Fig. 6 C, black bars). Suppression of NEEP21 had no effect up to 15 min, but then strongly retarded the decrease of internal Tf (white bars). Even after 2 h, there was still 46% of the maximal fluorescence at 15 min left. Fig. 6 D shows an antisense-transfected cell that is Tf positive (left), and a GFP-transfected cell
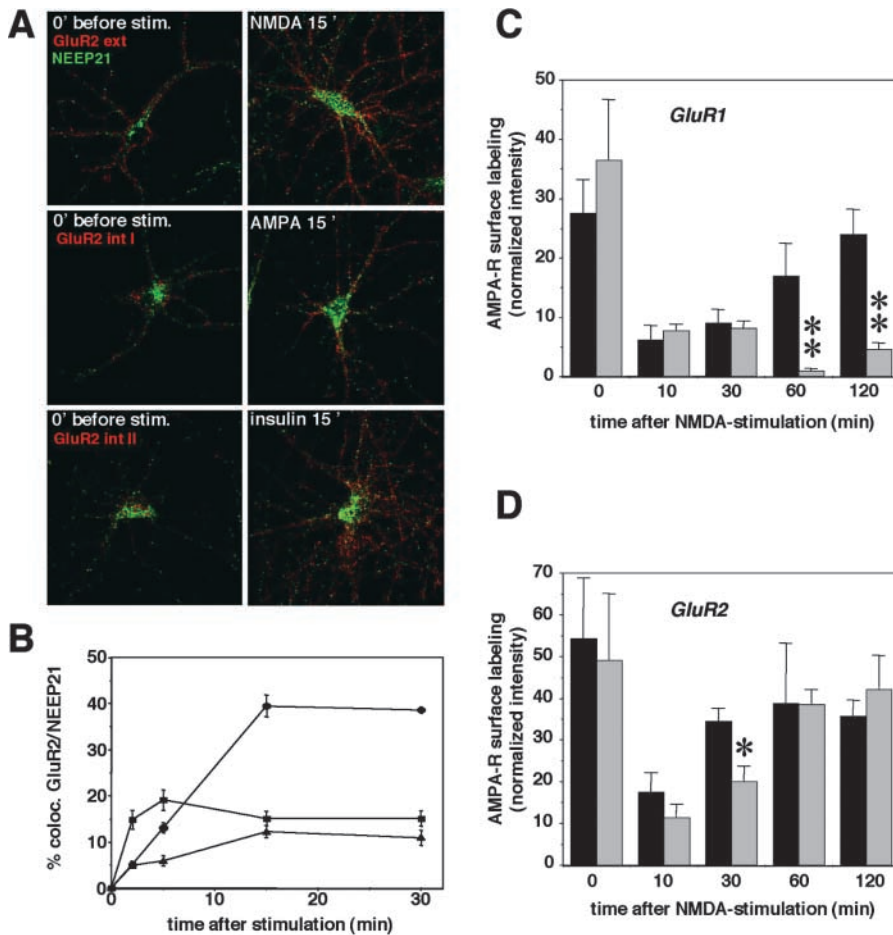
Figure 8. **NEEP21 is involved in AMPA receptor recycling.** (A) Left row, hippocampal neurons at DIV8 were incubated with an antibody against an extracellular epitope of GluR2 (red). Cells were then fixed and labeled with Cy3 secondary IgG without detergent (GluR2 ext) or with Cy5 secondary IgG without detergent and then Cy3 secondary IgG with detergent (GluR2 int), and immunolabeling for NEEP21 (green). Right row, as for GluR2 int., but with stimulation with either 50 μM NMDA, 100 μM AMPA (both 2 min) or 500 nM insulin (15 min), and further incubation at 37°C up to 15 min before fixation. (B) Quantification using the NIH image software of colocalization on confocal sections as in A (NMDA, ●; AMPA, ■; insulin, ▲). (C) Down-regulation of NEEP21 retards GluR1 recycling. Hippocampal neurons (DIV10) transfected with either GFP (black bars) or antisense (gray bars) constructs were stimulated for 2 min with NMDA, and were further incubated for the indicated times before fixation and surface labeling using an anti-GluR1 antibody against an extracellular domain. Fluorescence intensity was quantified. (D) GluR2 cycling was analyzed as in C. Typical experiments out of three are shown in C and D, and 5–10 cells per condition were analyzed by a Student *t* test. Significant differences at *P* < 0.01 (double asterisk) and at *P* < 0.02 (single asterisk) are indicated. Error bars are SEM.

that is Tf negative (right) at 60 min. Absence of endogenous NEEP21 verified antisense suppression (bottom row). In contrast, overexpression of NEEP21 resulted in a significant increase in internalization at 3 and 5 min, and a more rapid decrease at 30 and 60 min (Fig. 6 C, gray bars). In all conditions, the same maximal internalization was reached at 15 min. Transfection of GFP, NEEP21-EE, or antisense did not affect the steady-state distribution of TfR (unpublished data).

In an equivalent assay using peroxidase-conjugated Tf (HRP-Tf), we confirmed the accelerated internalization upon NEEP21 transfection. We used the rat pancreatic β cell line HIT-T15 because of its high transfection efficiency, and a low binding of human Tf to nontransfected control cells. When HRP activity was measured in cell lysates, we found that cells overexpressing NEEP21 (Fig. 6 E, gray bars) had significantly more Tf internalized at 3 min (20.64% vs. 13.25%; *P* < 0.001), as well as at 8 min (32.67% vs. 21.64%; *P* < 0.001), than the vector-transfected cells (black bars).

To verify whether cycling of other, unrelated membrane proteins is also modulated in PC12 cells by NEEP21, we tested recycling of the neuronal adhesion molecule L1 (Kamiguchi and Lemmon, 2000). Costaining shows significant colocalization of internal L1 in NEEP21-positive endosomes (Fig. 6 F, arrowheads). By surface labeling using an extracellularly binding anti-L1 antibody on PC12 cells (preblocked at 0-min time point), we found that antisense transfection (Fig. 6 G, white bars) significantly retarded reinsertion of L1 into the plasma membrane compared with GFP transfection

(black bars; *P* < 0.01 at 45, 60, and 120 min). There was a marginal acceleration by overexpression at 30 and 60 min (gray bars; *P* < 0.012). These results indicate that NEEP21 is essential for correct receptor cycling in PC12 cells. It also suggests that it might act on a large range of different receptors.

NEEP21 is a somatodendritic protein involved in AMPA receptor cycling

We next analyzed the localization of NEEP21 to specific neuronal domains using markers of the somatodendritic compartment (MAP2), axons (Tau, SNAP-25), and SVs (SV2, synaptophysin). NEEP21-positive puncta were present in the cell body and processes (Fig. 7, A, D, G, J, and M), which in all cases were positive for MAP2 (Fig. 7, B and overlay in C). In contrast, fibers outlined by Tau (Fig. 7 E) and SNAP-25 (Fig. 7 H) did not overlap with NEEP21. This shows that NEEP21 localizes to the somatodendritic compartment of neurons. To rule out that the NEEP21-labeled structures were presynaptic boutons, we costained for SV2 (Fig. 7 K) and synaptophysin (Fig. 7 N). Although the signals were clearly segregated, the processes outlined by NEEP21 were often surrounded by the synaptic vesicle markers. This is evident in the selected areas of Fig. 7, J and K, and M and N, which are enlarged in the overlays, L and O, respectively. This suggests that there are synapses onto NEEP21-containing dendrites.

Internalization of AMPA receptors into endosomal compartments or their recruitment to the cell surface modu-

lates synaptic strength (Carroll et al., 1999; Beatti et al., 2000; Ehlers, 2000; Lin et al., 2000). Given the somatodendritic localization of NEEP21, we analyzed its colocalization with AMPA receptors. We chose the subunit GluR2 because a monoclonal antibody against its extracellular domain was available to us. It has been suggested that internalized AMPA receptors take different trafficking routes depending on the stimulus (Ehlers, 2000; Lin et al., 2000). Therefore, we prebound the anti-GluR2 antibody to hippocampal neurons, and then stimulated them with NMDA or AMPA for 2 min or insulin for 15 min (expect time point at 2 min). At different times after stimulation, cells were fixed for immunolabeling. Fig. 8 A illustrates typical cells before stimulation (left row, top image, external GluR2; middle and bottom images, internal GluR2) and after 15 min of the indicated stimuli (right row, internal GluR2). Fig. 8 B shows quantification of colocalization between NEEP21 and GluR2, representing 10 cells at each point. At 2 min there was only 5.1 and 4.9% colocalization upon NMDA and insulin stimulation, respectively, whereas AMPA caused 14.8% colocalization, probably because AMPA binds directly to AMPA receptor. At later time points, colocalization after NMDA treatment increased strongly to 39.5% at 15 min, and 38.6% at 30 min, whereas colocalization after AMPA or insulin stimulation remained <20%. All three stimuli caused a steady increase in internal GluR2 staining, verifying efficient stimulations (unpublished data). This suggests that mainly NMDA stimulation directs AMPA receptors to NEEP21-positive compartments.

It has been proposed that AMPA receptors enter a recycling pathway after NMDA stimulation (Ehlers, 2000). Therefore, we analyzed whether suppression of NEEP21 affects cycling of AMPA receptors after NMDA stimulation in hippocampal neurons. We first chose GluR1 because it has been suggested that GluR1 trafficking is regulated (Passafaro et al., 2001; Shi et al., 2001). Cells transfected with either GFP (control) or antisense (suppression) were fixed at different times after stimulation. Surface AMPA receptors were then stained without permeabilization using an antibody against the extracellular domain of GluR1 (Fig. 8 C). Fluorescence intensities were equal for both transfections before stimulation (100%). After stimulation, the signals decreased at 10 min to 22.2 (control, black bars) and 21.1% (antisense, gray bars), reflecting equal receptor internalization, and remained low until 30 min (32.4 and 22.3%). Surface labeling in GFP-transfected cells increased again at 60 min to 61.6%, and at 120 min to 86.9%. In contrast, labeling in antisense-transfected cells remained significantly lower ($P < 0.01$) at 60 (2.6%) and 120 min (12.7%). When performing the equivalent experiment for GluR2 (Fig. 8 D), we observed in control cells a faster cycling than for GluR1 (Fig. 8, compare D and C), in agreement with their reported time courses (Passafaro et al., 2001). Upon suppression of NEEP21, recycling of GluR2 was retarded at 30 min (40.8%) compared with control cells (63.3%, $P < 0.02$). These results indicate that NEEP21 down-regulation delays recycling of AMPA receptors after NMDA stimulation of hippocampal neurons.

Discussion

Although correct cycling of neuronal plasma membrane receptors is essential for their proper function (Buckley et al., 2000), endosomal compartments of neurons and their potentially neuron-specific proteins remain poorly characterized. Using syntaxin 13 as a bait, we identified a neuronal protein, 1A75/p21, of so far unknown function. We suggest the name NEEP21 because: (a) it localizes to Rab4-positive, wortmannin-sensitive endosomes of the somatodendritic neuronal compartment; (b) its overexpression or suppression modulate Tf and L1 cycling; (c) NMDA-stimulation internalizes surface-labeled GluR2 into NEEP21-positive endosomes; and (d) NEEP21 suppression delays GluR1 recycling after NMDA stimulation.

NEEP21, also called 1A75 (Sutcliffe et al., 1983), p21 (Saberan-Djoneidi et al., 1998), or D4S234 (Carlock et al., 1996), as well as the highly homologous p19 (Saberan-Djoneidi et al., 1995), are proteins of so far unknown function, strongly enriched in neurons. NEEP21 is 98.4% identical between mouse and human, and 99.5% between rat and mouse. Two EST sequences (AJ394144 and AJ393704) indicate the existence of a chicken homologue 88% identical to human NEEP21. A predicted α-helix between aa 164–181 in its cytosolic COOH-terminal tail might be involved in protein complex formation. The 24-kD protein calcyon, which regulates dopamine receptors D1 (Lezcano et al., 2000), is 37% identical to NEEP21. It has the same membrane orientation as we determined here for NEEP21.

NEEP21 significantly colocalized with syntaxin 13, Rab4, TfR, and internalized Tf, but not with a late endosome marker. In addition, overexpression or down-regulation of NEEP21 modulated Tf cycling. Therefore, we conclude that NEEP21 is mainly localized to an early endosomal population. Its colocalization with the TGN marker TGN38 in the perinuclear region might be due to either NEEP21 during biosynthesis, or its presence in perinuclear endosomes close to Golgi compartments (Gruenberg and Maxfield, 1995), or a subpopulation of NEEP21 localized to TGN. Similar to our staining, Saberan-Djoneidi et al. (1998) identified NEEP21/p21 in a punctated staining in the juxtanuclear region and in the periphery of neurons. Although double labeling was not performed, the authors interpreted the staining as Golgi complex.

Using double labelings and drug treatments, we analyzed in detail the NEEP21 localization along the endosomal pathway. Rab5 is involved in endocytosis (McLauchlan et al., 1998) and vesicle fusion on EEs (Gorvel et al., 1991), Rab4 in trafficking from EE to the plasma membrane (van der Sluijs et al., 1992) and presumably also to REs (Nagelkerken et al., 2000), and Rab11 in trafficking through REs (Ullrich et al., 1996). Recent data from imaging in living cells (Sonnichsen et al., 2000) and from immunoisolation of endosomal populations (Trischler et al., 1999) suggest a wortmannin-sensitive Rab5/Rab4 domain and a BFA-sensitive Rab4/Rab11 domain along the endosomal pathway. We found here that NEEP21 colocalized significantly with Rab4-positive endosomes, whereas little overlap was observed with Rab5- and EEA1-labeled endosomes in PC12 cells. In addition, wortmannin, but not BFA, relocalized NEEP21, to-

gether with TfR in primary neurons. Together with the delayed colocalization with Tf, we propose that NEEP21 localizes mainly to a Rab4-positive domain on EE involved in transport to RE or to the plasma membrane. The GTPase-deficient mutant Rab5Q79L causes enlarged endosomes by an increased fusion of endocytosed vesicles with EE (Stenmark et al., 1994). NEEP21, located primarily to a Rab4-domain of EE, would obviously be affected by Rab5Q79L-induced EE enlargement.

Syntaxin 13 was detected on tubular RE (Prekeris et al., 1998) which could be enriched using an anti-Rab11 antibody, whereas lower amounts were also detected in anti–Rab5-enriched endosomes (Trischler et al., 1999). Moreover, syntaxin 13 has been identified in a complex with the Rab5-effectors Rabaptin-5 and EEA1 (McBride et al., 1999). Therefore, syntaxin 13 might act on REs and EEs, where it could interact with NEEP21. Although we did not detect EEA1 or Rabaptin-5 in anti-NEEP21 immunoprecipitations (IPs) (unpublished data), this does not rule out that NEEP21 is involved in the formation of the labile EEA1/Rabaptin/syntaxin 13 complex (McBride et al., 1999).

Overexpression of NEEP21 caused a significant acceleration of Tf cycling, whereas antisense-mediated down-regulation lead to an inhibition of recycling. In light of the described NEEP21 localization, faster decrease of internal Tf upon overexpression is most probably an accelerated recycling of Tf to RE or to the plasma membrane. This could indirectly stimulate earlier steps of the cycle causing faster internalization. Upon NEEP21 down-regulation, Tf might correctly internalize into EEs, but an inhibited transport to the plasma membrane or to REs might retain Tf for longer time in endosomal compartments.

In contrast to other known endosomal proteins, NEEP21 has only been detected in neurons and, at a lower level, in testis (Sutcliffe et al., 1983; Saberan-Djoneidi et al., 1998). Therefore, it is probably not engaged in ubiquitous endosomal trafficking. In primary neurons, NEEP21 localized to processes positive for a dendritic marker, but negative for axonal markers. Consequently, the function of NEEP21 must be specific to endosomal trafficking of somatodendritic membrane proteins of neurons. Recent studies have proven the importance of AMPA receptor internalization for the expression of long-term depression, a form of synaptic plasticity (Carroll et al., 1999; Beatti et al., 2000). The endocytosed receptors are detected in syntaxin 13– (Lin et al., 2000) and Rab4-positive (Ehlers, 2000) compartments. We found here that among the three stimuli applied, NMDA resulted in the strongest colocalization between the AMPA receptor subunit GluR2 and NEEP21. In addition, antisense-mediated down-regulation of NEEP21 retarded recycling of GluR1 (and marginally of GluR2) after NMDA application. Because NMDA receptor activation has been proposed to cause AMPA receptor internalization with subsequent recycling to the plasma membrane (Ehlers, 2000), our results indicate that NEEP21 is an important component in the machinery necessary for AMPA receptor recycling. Expression of NEEP21 mRNA (Sutcliffe et al., 1983; Saberan-Djoneidi et al., 1998) and protein (present study) is highest during the first postnatal week. AMPA receptors are recruited into NMDA receptor-containing synapses during postnatal de-

velopment, with a subsequent switch of receptor subunits (Pickard et al., 2000; Zhu et al., 2000). Our results correlate well with a role of NEEP21 in such a recruitment and/or subunit exchange during synaptogenesis.

Suppression of NEEP21 not only affected AMPA receptor cycling, but also TfR and L1 in PC12 cells. Because these three molecules are rather divergent plasma membrane proteins, NEEP21 probably acts on a larger range of receptors than only on one specific type. Although further studies will have to clarify the precise function of NEEP21, this protein is, to our knowledge, the first neuronal protein with a distinct localization in the early endosomal pathway and with a function in the cycling of neuronal receptors.

Materials and methods

Antibodies

A polyclonal antiserum was raised against a peptide spanning aa 7–23 of NEEP21 (Eurogentec) and affinity purified using Affigel 10 (Bio-Rad Laboratories). It was used at 1:300 for immunofluorescence (IF) and 1:6,000 for Western blots (W). We used antibodies against the following antigens: (a) polyclonal, syntaxin 13 (W 1:6,000; IF 1:200; Hirling et al., 2000); TGN38 (IF 1:500, a gift of Dr. G. Banting [University of Bristol, Bristol, UK]); GluR1 (IF 1:10; Calbiochem); and L1 (IF 1:4,000, a gift of Dr. V. Lemmon [Case Western University, Cleveland, OH]); and (b) monoclonal, myc-tag (9E10 hybridoma supernatant; IF 1:20; W 1:10); EE-tag (supernatant; IF 1:30; W 1:2,000; Grussenmeyer et al., 1985); Tau (supernatant; IF 1:10, provided by Dr. B. Riederer [University of Lausanne, Lausanne, Switzerland]); SV2 (IF 1:500; W 1:5,000; developed by Dr. K. Buckley, obtained from Developmental Studies Hybridoma Bank, Iowa City, IA); MAP2 (IF 1:300; Sigma-Aldrich); SNAP-25 (IF, W 1:2,000; Sternberger Monoclonals); rat TfR (IF 1:500; Chemicon); αSNAP (W 1:2,000, a gift of Dr. R. Jahn [Max-Planck Institute, Göttingen, Germany]); Rab4, Rab11, and EEA1 (IF 1:300; W 1:2,000; Transduction Labs); GluR2 (IF, 1:250; Chemicon); lysobisphosphatidic acid (clone 6C4; IF 1:50, a gift of Dr. J. Gruenberg [University of Geneva, Geneva, Switzerland]); and synaptophysin (IF 1:250; Synaptic Systems). We applied HRP- (W 1:2,000; Calbiochem); Cy3-, Cy5- (IF 1:200; Jackson ImmunoResearch Laboratories), and Oregon Green–coupled (IF 1:200; Molecular Probes Inc.) secondary anti–mouse and anti–rabbit IgG.

Identification of NEEP21

Immunoaffinity chromatography and Western blots were performed as described (Hirling et al., 2000) with modifications: (a) An anti–syntaxin 13 column was used; (b) membrane pellets were lysed in B/1% Triton X-100 (T)/0.1 M KCl (K)/10 μM Taxol (Sigma-Aldrich) to reduce tubulin content; (c) columns were washed by 20 vol of B/1% T/0.1 M K, 2 vol of B/0.2% T/0.1 M K, 2 vol of B/0.2% T/0.5 M K, 1 vol of B/0.2% T/1 M K, and 1 vol of B/0.2% T/0.1 M K; and (d) purifications from 21 g of P3 rat brain were pooled, and a band at 21 kD was cut out from gel for peptide sequencing. A single peak contained a sequence matching the brain-specific clone 1A75/p21 (Sutcliffe et al., 1983; Saberan-Djoneidi et al., 1998). We amplified, by PCR, a full-length mouse clone using oligo-dT–primed mouse brain cDNA. To express tagged protein, the myc-his–coding sequence between XbaI and PmeI of pcDNA3.1/myc-his.B (Invitrogen) was replaced by GAGTACATGCCCATGGAGTGA coding for the EE tag EYMPMEstop (Grussenmeyer et al., 1985). The cDNA of full-length or deleted mouse 1A75, which we propose to name NEEP21, was subcloned by PCR into EcoRI/XhoI upstream of this EE tag, a gift of Dr. D. Lavery (ICBM, Lausanne, Switzerland). To express NEEP21 antisense RNA, its cDNA was subcloned by PCR in the reverse direction into pcDNA3 between BamHI and EcoRI, downstream of the GFP cDNA and additional stop codons (herein called pcDNA3-antisense). The cDNAs of Rab5–wild-type and -Q79L (Stenmark et al., 1994) were subcloned by PCR as BamHI/EcoRI fragments downstream of a myc tag in pcDNA3.

For IPs, polyclonal and monoclonal antibodies were crosslinked by 20 mM dimethylpimelimidate to protein A– and protein G–Sepharose, respectively (Amersham Pharmacia Biotech). P3 membrane extract (160 μg) was incubated with 10-μl beads for 4 h, and washed and eluted as above. Transfected COS-7 cells were lysed in buffer B/100 mM K/1% T, centri-

---

fuged at 20,000 *g*, and incubated with antibody beads for 4 h. Beads were washed (B/100 mM K/0.2% T) and eluted as above. Cortical neurons were lysed in PBS/0.5% T. Protein concentrations were determined by the Bradford technique (Bio-Rad Laboratories) and Coomassie blue–stained SDS-PAGE. For trypsin digestions, PC12 cells were lysed by seven passages through a 25-G needle, and centrifuged at 3,000 *g* for 5 min. The supernatant (40 μg) was incubated for 1 h either without additions, or with 4 μg trypsin, or with trypsin and 0.5% T, followed by Western blot. All preparations were done at 4°C.

Cell culture and immunocytochemistry

PC12ES cells were processed as described (Hirling et al., 2000). COS-7 cells were grown in DME/10% FCS and transfected by Fugene (Roche).

Cortical rat neurons were prepared as described (Hirling et al., 2000). Hippocampal neurons were prepared from P0 rats. Hippocampi without dentate gyri were dissociated with papain and triturated using a glass pipette. After centrifugation at 400 *g* for 2 min, cells were plated at 150,000 cells per 35-mm dish containing poly-D-lysin/laminin-coated borosilicate coverslips in DME/10% FCS. Medium was changed after 3 h to Neurobasal/B27 medium. Neurons were transfected according to Xia et al. (1996) by the calcium-phosphate technique 2 d before immunocytochemistry. DNA (4 μg) in 60 μl CaCl$_2$ was mixed with 60 μl 2 × HBS, pH 7.0, and added to one culture dish (35 mm) for 30 min, followed by glycerol shock for 1 min.

For immunocytochemistry (Hirling et al., 2000), cultures were fixed in 4% paraformaldehyde/4% sucrose. For labeling of Rab proteins or of LBPA, PC12 cells were prepermeabilized in PBS for 150 s with 0.04% digitonin, or for 30 min in 0.05% saponin, respectively. FITC- or rhodamin-conjugated human Tf (0.025 mg/ml; Molecular Probes) was added to cells transfected with pcDNA3-hTfR (human TfR, a gift of Dr. L. Kühn (ISREC, Epalinges, Switzerland), Epalinges, Switzerland) in serum-free medium for 20 min at 4°C, followed by incubation without Tf for the indicated times at 37°C. For L1 surface labeling, transfected PC12 cells were incubated on ice for 1 h with an extracellularly binding anti-L1 antibody, and then for 1 h with Cy5 secondary IgG. Then cells were incubated at 37°C for the indicated times, fixed, and incubated without detergent with anti-L1, and then with Cy3 secondary IgG. For drug treatments, cortical neurons at DIV3 were treated for 60 min with 5 μg/ml BFA or with 100 nM wortmannin before immunolabeling. For labeling of internalized GluR2, hippocampal neurons after DIV8 were incubated for 1 h at 37°C with TTX (2 μM) and for 30 min with TTX and anti-GluR2 against an extracellular epitope. After washing, neurons were stimulated with 100 μM AMPA or 50 μM NMDA for 2 min, or with 500 nM insulin for 15 min (expect for time point at 2 min), and further incubated at 37°C for the indicated times. Neurons were fixed and Cy5-anti–mouse IgG was added for 30 min without detergent (to block noninternalized GluR2); then anti-NEEP21 was added with detergent, followed by Cy3-anti–mouse IgG and Oregon Green anti–rabbit IgG. To measure recycling of GluR1 or GluR2, hippocampal neurons, transfected with either pcDNA3-GFP or pcDNA3 antisense, were preincubated on DIV10 for 1 h with TTX (2 μM) before stimulation with TTX/NMDA (50 μM) for 2 min. Cells were rinsed and incubated at 37°C in medium/TTX before fixation and immunolabeling without detergent using anti-GluR1 or -GluR2 antibodies (both against extracellular domains). Immunostained cells were analyzed on a Leica TCSNT confocal microscope and processed with Adobe® Photoshop® (v. 5.5).

Tf cycling assays

PC12 cells were cotransfected with pcDNA3 coding hTfR and either NEEP21-EE, antisense, or GFP. After 2 d of differentiation, cells were incubated on ice for 30 min with 25 ng/ml rhodamin-Tf. Cells were then rinsed with medium and shifted to 37°C for the indicated times, and washed twice with PBS/30 mM glycine, pH 2.5, and twice with PBS, followed by immunocytochemistry for NEEP21. To measure Tf internalization biochemically, HRP-conjugated human Tf (HRP-Tf; Pierce Chemical Co.) was used on the hamster pancreatic β cell line HIT-T15. Cells were grown in RPMI 1640/10% FCS/2.05 mM L-glutamine/32.5 μM glutathione/10 mM selenic acid, and electroporated with pcDNA3-hTfR and either pcDNA3 or pcDNA3-NEEP21-EE. Cells were incubated on ice for 60 min with 10 ng/ml HRP-Tf. Cells were then rinsed and either lysed with PBS/0.5% T, followed by spectrophotometrical peroxidase assay using TMB substrate (Sigma-Aldrich) (corresponds to 100% bound Tf), or shifted to 37°C for 3 or 8 min. These cells were washed on ice with PBS/glycine, pH 2.5, before lysis and peroxidase assay (corresponds to the percentage of internalized Tf). Results from five independent experiments were cumulated and statistically analyzed by a two-way analysis of variance test.

Quantitative image analysis

All experiments were done at least three times. Three confocal sections covering the whole thickness of the cell were acquired with identical parameters, and in each case the middle section was used for quantification. For colocalization, two separate confocal images for the red (1) and green (2) channels were acquired. The threshold was set at a fixed value. The intersection image of the merged red and green channels was separated into red (3) and green (4) channels corresponding to the double-labeled pixels. Channels 1–4 were analyzed using NIH image software for mean pixel intensity and number of labeled pixels. We then added the values from channels 1 and 2 (corresponding to 100% in Fig. 8 B; pixels being red or green), and from the intersected red (3) and green (4) channels (corresponds to colocalization; pixels being red and green). Values from 10 cells per condition were statistically analyzed by a *t* test (double asterisks, $P < 0.01$). For quantification of surface GluR labeling, the threshold was adjusted by NIH image to a level that suppressed all noncellular signals to two pixels per cm^2 (corresponding to 0.3% of all pixels) to have a minimal visual background density. The average pixel intensity (normalized intensity) was determined by dividing the sum of all pixel intensities by the number of labeled pixels above threshold. Between 5 and 10 cells per condition were measured, and the results were analyzed by a *t* test (double asterisks, $P < 0.01$; single asterisks, $P < 0.02$). Quantification of Tf and L1 cycling was performed as described for GluR. Between 50 and 150 cells per condition were measured and the results were analyzed by a *t* test (double asterisks, $P < 0.01$).

References

Beatti, E.C., R.C. Carroll, X. Yu, W. Morishita, H. Yasuda, M. von Zastrow and R.C. Malenka. 2000. Regulation of AMPA receptor endocytosis by a signaling mechansim shared with LTD. *Nat. Neurosci.* 3:1291–1200.

Buckley, K.M., H.E. Melikian, C.J. Provoda, and M.T. Waring. 2000. Regulation of neuronal function by protein trafficking: a role for the endosomal pathway. *J. Physiol.* 525:11–19.

Carlock, L., T. Vo, M. Lorincz, P.D. Walker, D. Bessert, D. Wisniewski, and J.C. Dunbar. 1996. Variable subcellular localization of a neuron-specific protein during NTera 2 differentiation into post-mitotic human neurons. *Molec. Brain Res.* 42:202–212.

Carroll, R.C., D.V. Lissin, M. von Zastrow, R.A. Nicoll, and R.C. Malenka. 1999. Rapid redistribution of glutamate receptors contributes to long-term depression in hippocampal cultures. *Nat. Neurosci.* 2:454–460.

Dailey, M.E., and P.C. Bridgman. 1993. Vacuole dynamics in growth cones: correlated EM and video observations. *J. Neurosci.* 13:3375–3393.

Diefenbach, T.J., P.B. Guthrie, H. Stier, B. Billups, and S.B. Kater. 1999. Membrane recycling in the neuronal growth cone revealed by FM1-43 labeling. *J. Neurosci.* 19:9436–9444.

Ehlers, M.D. 2000. Reinsertion or degradation of AMPA receptors determined by activity-dependent endocytic sorting. *Neuron.* 28:511–525.

Gorvel, J.P., P. Chavrier, M. Zerial, and J. Gruenberg. 1991. Rab5 controls early endosome fusion in vitro. *Cell.* 64:915–925.

Grimes, M.L., J. Zhou, E.C. Beattie, E.C. Yuen, D.E. Hall, J.S. Valletta, K.S. Topp, J.H. LaVail, N.W. Bunnett, and W.C. Mobley. 1996. Endocytosis of activated TrkA: evidence that nerve growth factor induces formation of signaling endosomes. *J. Neurosci.* 16:7950–7964.

Gruenberg, J., and F.R. Maxfield. 1995. Membrane transport in the endocytic pathway. *Curr. Opin. Cell Biol.* 7:552–563.

Grussenmeyer, T., K.H. Scheidtmann, M.A. Hutchinson, W. Eckhart, and G. Walter. 1985. Complexes of polyoma virus medium T antigen and cellular proteins. *Proc. Natl. Acad. Sci. USA.* 82:7952–7954.

Hirling, H., P. Steiner, C. Chaperon, R. Marsault, R. Regazzi, and S. Catsicas. 2000. Syntaxin 13 is a developmentally regulated SNARE involved in neu-

rite outgrowth and endosomal trafficking. *Eur. J. Neurosci.* 12:1913–1923.

Kamiguchi, H., and V. Lemmon. 2000. Recycling of the cell adhesion molecule L1 in axonal growth cones. *J. Neurosci.* 20:3676–3686.

Kobayashi, T., E. Stang, K.S. Fang, P. de Moerloose, R.G. Parton, and J. Gruenberg. 1998. A lipid associated with the antiphospholipid syndrome regulates endosome structure and function. *Nature.* 392:193–197.

Lezcano, N., L. Mrzljak, S. Eubanks, R. Levenson, P. Goldman-Rakic, and C. Bergson. 2000. Dual signaling regulated by calcyon, a D1 dopamine receptor interacting protein. *Science.* 287:1660–1664.

Lin, J.W., J. William, K. Foster, S.H. Lee, G. Ahmadian, M. Wyszynski, Y.T. Wang, and M. Sheng. 2000. Distinct molecular mechanisms and divergent endocytotic pathways of AMPA receptor internalization. *Nat. Neurosci.* 3:1282–1290.

Lippincott-Schwartz, J., L. Yuan, C. Tipper, M. Amherdt, L. Orci, and R.D. Klausner. 1991. Brefeldin A's effects on endosomes, lysosomes, and the TGN suggest a general mechanism for regulating organelle structure and membrane traffic. *Cell.* 67:601–616.

Malide, D., and S.W. Cushman. 1997. Morphological effects of wortmannin on the endosomal system and GLUT4-containing compartments in rat adipose cells. *J. Cell Sci.* 110:2795–2806.

McBride, H.M., V. Rybin, C. Murphy, A. Giner, R. Teasdale, and M. Zerial. 1999. Oligomeric complexes link Rab5 effectors with NSF and drive membrane fusion via interactions between EEA1 and syntaxin 13. *Cell.* 98:377–386.

McLauchlan, H., J. Newell, N. Morrice, A. Osborne, M. West, and E. Smythe. 1998. A novel role for Rab5-GDI in ligand sequestration into clathrin-coated pits. *Curr. Biol.* 8:34–45.

Nagelkerken, B., E. Van Anken, M. Van Raak, L. Gerez, K. Mohrmann, N. Van Uden, J. Holthuizen, L. Pelkmans, and P. Van Der Sluijs. 2000. Rabaptin4, a novel effector of the small GTPase Rab4a, is recruited to perinuclear recycling vesicles. *Biochem. J.* 346:593–601.

Passafaro, M., V. Piech, and M. Sheng. 2001. Subunit-specific temporal and spatial patterns of AMPA receptor exocytosis in hippocampal neurons. *Nat. Neurosci.* 4:917–926.

Pickard, L., J. Noel, J.M. Henley, G.L. Collingridge, and E. Molnar. 2000. Developmental changes in synaptic AMPA and NMDA receptor distribution and AMPA receptor subunit composition in living hippocampal neurons. *J. Neurosci.* 20:7922–7931.

Prekeris, R., J. Klumperman, Y.A. Chen, and R.H. Scheller. 1998. Syntaxin 13 mediates cycling of plasma membrane proteins via tubulovesicular recycling endosomes. *J. Cell Biol.* 143:957–971.

Rothman, J.E. 1994. Mechanisms of intracellular protein transport. *Nature.* 372:55–63.

Saberan-Djoneidi, D., I. Marey-Semper, R. Picart, J.M. Studler, C. Tougard, J. Glowinski, and M. Levi-Strauss. 1995. A 19-kDa protein belonging to a new family is expressed in the Golgi apparatus of neural cells. *J. Biol. Chem.* 270:1888–1893.

Saberan-Djoneidi, D., R. Picart, D. Escalier, M. Gelman, A. Barret, C. Tougard, J. Glowinski, and M. Levi-Strauss. 1998. A 21-kDa polypeptide belonging to a new family of proteins is expressed in the Golgi apparatus of neural and germ cells. *J. Biol. Chem.* 273:3909–3914.

Shi, S.H., Y. Hayashi, J.A. Esteban, and R. Malinow. 2001. Subunit-specific rules governing AMPA receptor trafficking to synapses in hippocampal pyramidal neurons. *Cell.* 105:331–343.

Sonnichsen, B., S. De Renzis, E. Nielsen, J. Rietdorf, and M. Zerial. 2000. Distinct membrane domains on endosomes in the recycling pathway visualized by multicolor imaging of Rab4, Rab5 and Rab11. *J. Cell Biol.* 149:901–913.

Spiro, D.J., W. Boll, T. Kirchhausen, and M. Wessling-Resnick. 1996. Wortmannin alters the transferrin receptor endocytic pathway in vivo and in vitro. *Mol. Biol. Cell.* 7:355–367.

Stenmark, H., R.G. Parton, O. Steele-Mortimer, A. Lutcke, J. Gruenberg, and M. Zerial. 1994. Inhibition of Rab5 GTPase activity stimulates membrane fusion in endocytosis. *EMBO J.* 13:1287–1296.

Sutcliffe, J.G., R.J. Milner, T.M. Shinnick, and F.E. Bloom. 1983. Identifying the protein products of brain-specific genes with antibodies to chemically synthesized peptides. *Cell.* 33:671–682.

Tang, B.L., A.E.H. Tan, L.K. Lim, S.S. Lee, D.Y.H. Low, and W.J. Hong. 1998. Syntaxin 12, a member of the syntaxin family localized to the endosome. *J. Biol. Chem.* 273:6944–6950.

Tooze, J., and M. Hollinshead. 1992. In AtT20 and HeLa cells brefeldin A induces the fusion of tubular endosomes and changes their distribution and some of their endocytic properties. *J. Cell Biol.* 118:813–830.

Trischler, M., W. Stoorvogel, and O. Ullrich. 1999. Biochemical analysis of distinct Rab5- and Rab11-positive endosomes along the transferrin pathway. *J. Cell Sci.* 112:4773–4783.

Ullrich, O., S. Reinsch, S. Urbe, M. Zerial, and R.G. Parton. 1996. Rab11 regulates recycling through the pericentriolar recycling endosome. *J. Cell Biol.* 135:913–924.

van der Sluijs, P., M. Hull, P. Webster, P. Male, B. Goud, and I. Mellman. 1992. The small GTP-binding protein Rab4 controls an early sorting event on the endocytic pathway. *Cell.* 70:729–740.

Wan, Q., Z.G. Xiong, H.Y. Man, C.A. Ackerley, J. Braunton, W.Y. Lu, L.E. Becker, J.F. MacDonald, and Y.T. Wang. 1997. Recruitment of functional GABA(A) receptors to postsynaptic domains by insulin. *Nature.* 388:686–690.

Xia, Z., H. Dudek, C.K. Miranti, and M.E. Greenberg. 1996. Calcium influx via the NMDA receptor induces immediate early gene transcription by a MAP kinase/ERK-dependent mechanism. *J. Neurosci.* 16:5425–5436.

Zhu, J.J., J.A. Esteban, Y. Hayashi, and R. Malinow. 2000. Postnatal synaptic potentiation: delivery of GluR4-containing AMPA receptors by spontaneous activity. *Nat. Neurosci.* 3:1098–1106.